Effect of solids retention times on the performance of thermal hydrolysis pretreated mesophilic anaerobic digestion system

A final report submitted to

Arlington Water Pollution Control Plant
(3402 S. Glebe Road, Arlington, VA 22202)
Email: Mstrawn@arlingtonva.us
&

HDR.Inc
(2650 Park Tower Drive #400, Vienna, VA 22180)
Email: brian.balchunas@hdrinc.com

By

Hao Luo and Zhiwu Wang

Department of Biological Systems Engineering, Virginia Tech

Email: wzw@vt.edu

Table of Contents

1 Introduction

Arlington Water Pollution Control Plant (AWPCP) has a master plan to install a thermal hydrolysis pretreatment (THP) system for high-rate mesophilic anaerobic digestion of the primary sludge (PS) and waste activated sludge (WAS) produced at AWPCP. Virginia Tech (VT) performed a series of THP/anaerobic digestion studies for AWPCP in 2019. The study exploited a 2L Parr pressure vessel to mimic the THP of blended PS and WAS at total solids (TS) of 3.7% and 7.4% and temperatures of 130, 150, and 170 ºC (Figures 1 and 2). There are two limitations in this previous study: 1) The time and temperature of the Parr pressure vessel cannot be controlled as accurately as those of the full-scale THP such as that from CAMBI^{TM}. This is because the Parr pressure vessel was not heated by steam and thus has to be placed in an oven for much longer time to ensure full penetration of heat into the sludge bed through conduction (Figure 2a); 2) The lab-scale 5L working volume mesophilic anaerobic digesters (ADs) as shown in Figure 2b were unable to mix THP sludge with TS greater than 9%. This is because these ADs were mixed by headspace gas recirculation as shown in Figure 2c which is not as powerful as mechanical mixing. This study was able to overcome these two previous limitations by using a steam heated small THP system (5 L capacity) provided by CAMBI^{TM} and mechanically mixed pilot-scale ADs designed by Prof. Matt Higgins at Bucknell University. The solids retention time (SRT) of AD was investigated as a new variable in this study, with the purpose of evaluating the effect of SRT on digester performance and optimizing the digester sizing criteria for full-scale design.

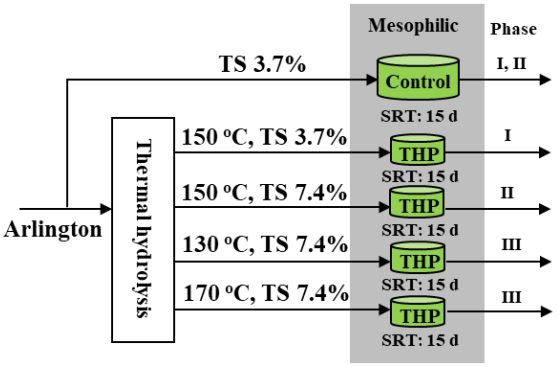

Figure 1. Summary of the experimental design in a previous Arlington project (Zhang et al., 2021a).

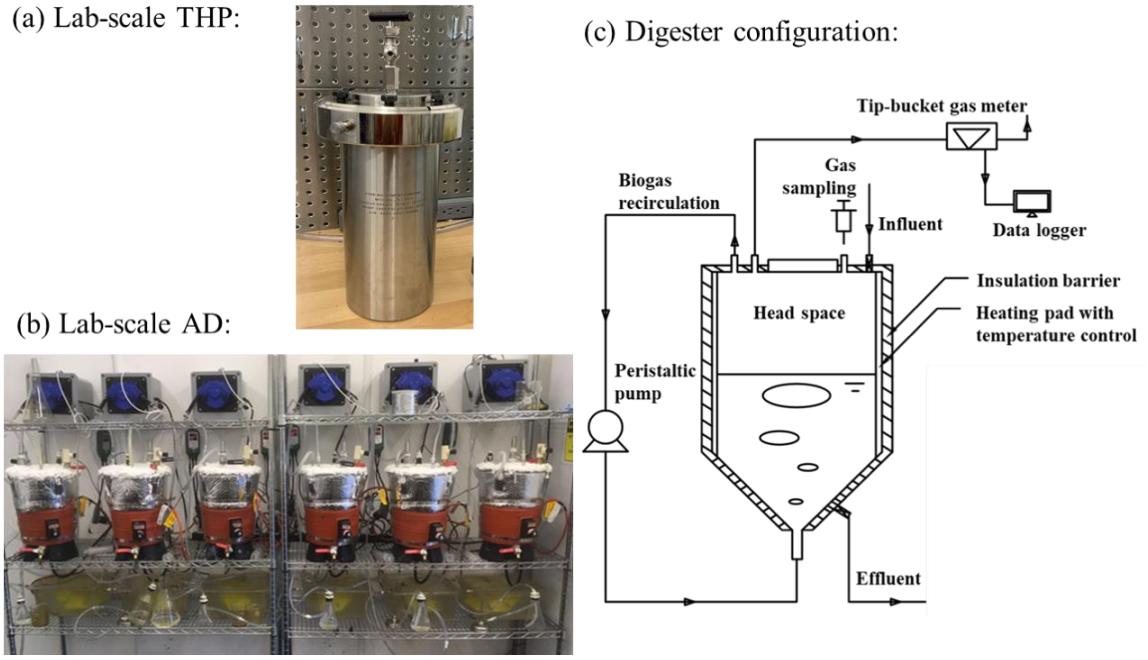

Figure 2. (a) A Parr pressure vessel used for the lab-scale THP; (b) The stainless-steel gas-mixed anaerobic digesters; (c) The digester configuration used in the previous study (Zhang et al., 2021a).

2 Materials and Methods

2.1 Experimental design

A process flow diagram of the THP - anaerobic digestion pilot system is provided in Figure 3. Dewatered PS/WAS cake collected from AWPCP with 30% TS was diluted to 16% TS prior to feeding into THP. The treated sludge from the THP unit was then used as influent for the pilot AD. The digester effluent was dewatered to generate filtrate and cake for the characterization. Chemical analyses were performed on the THP feed, AD influent, and effluent, as well as the filtrate and cake as shown in Figure 3.

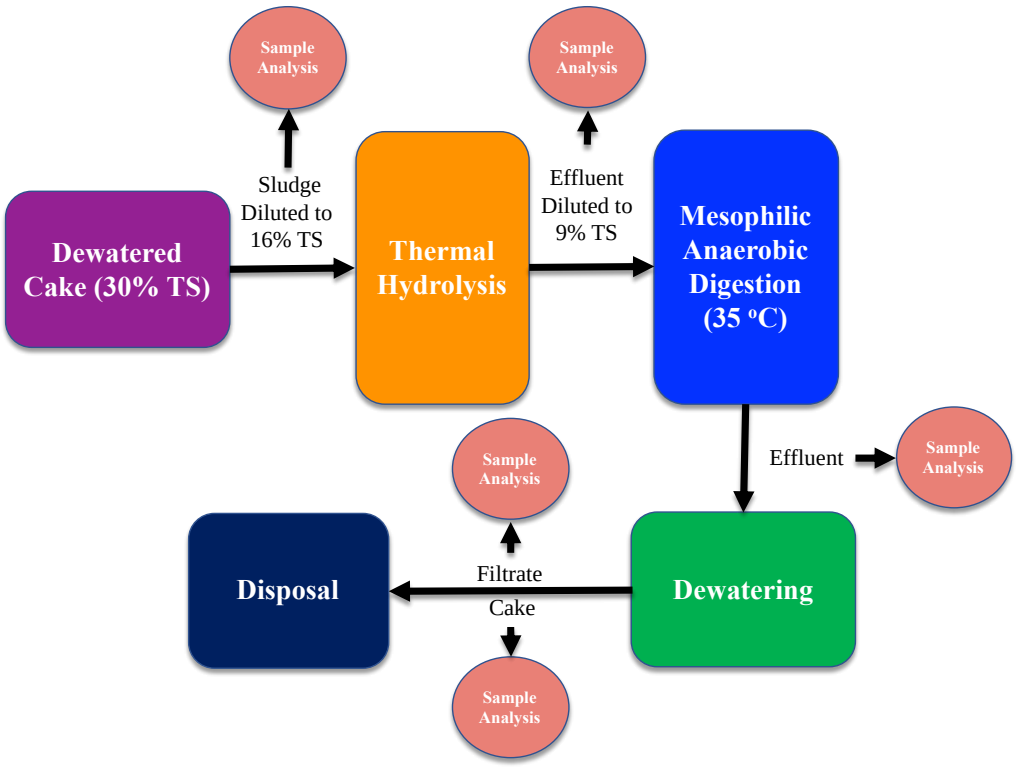

Figure 3. THP/AD System Flow Chart

2.2 THP and AD system

2.2.1 THP reactor

The THP setup for this pilot was purchased from CAMBI™ (Figure 4). The diluted sludge cake, at approximately 16% TS, was fed through the inlet tray at the top of the THP unit into the reactor tank. The steam from the steam generator was injected to quickly heat the dewatered sludge to a designated temperature (165 °C). After 30 min, the steam treated sludge was ejected through an orifice into the flash tank beneath the reactor tank (Figure 4). The treated sludge was then cooled to room temperature and diluted to approximately 9% prior to feeding into mesophilic ADs. The flow chart of THP operation procedures is shown in Figure 5.

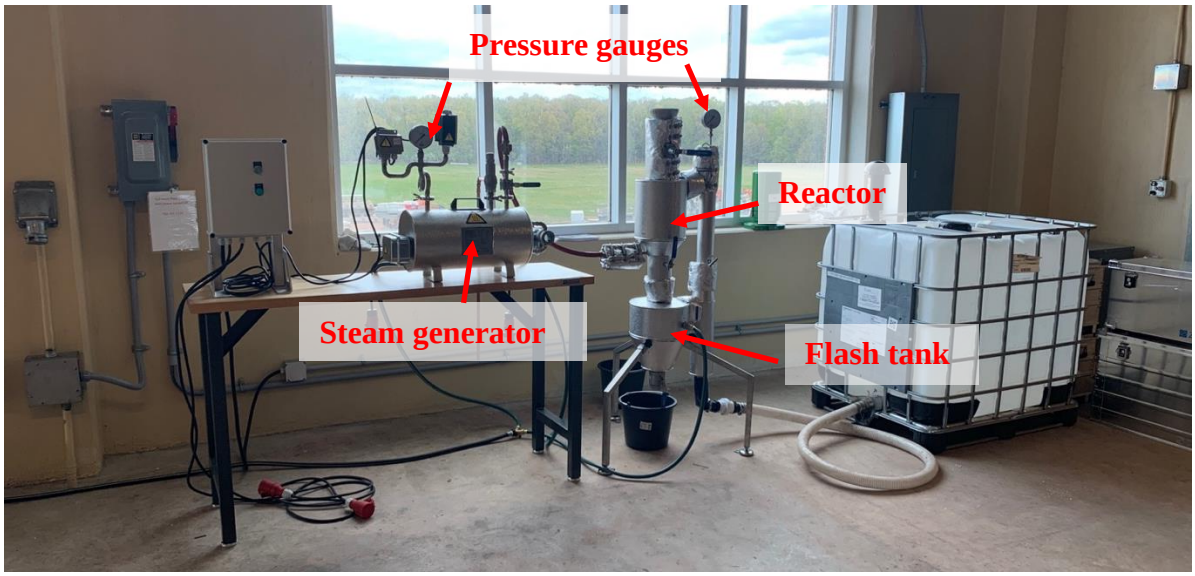

Figure 4. CAMBI™ Thermal Hydrolysis unit

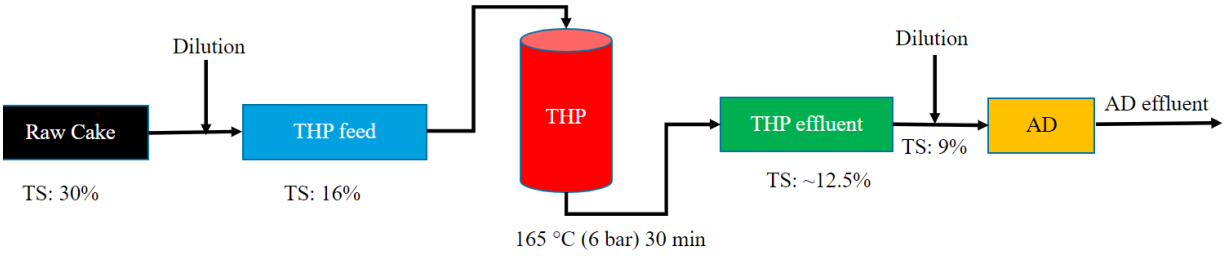

Figure 5. THP flow chart

2.2.2 AD tent system

Three mechanically mixed ADs as shown in Figure 6a were operated in parallel with temperature maintained at 36.5 ± 0.3 ˚C using a thermal tent as illustrated in Figure 6b. These ADs were inoculated with fresh effluent sludge from a full-scale THP-fed mesophilic AD at DC Water. The feed into the ADs was 9% TS. Blended sludge collected from AWPCP was processed through THP and then fed into three ADs to study the SRT effect on sludge anaerobic digestibility. The SRTs for these three digesters were set at 10, 12.5, and 15 days, respectively.

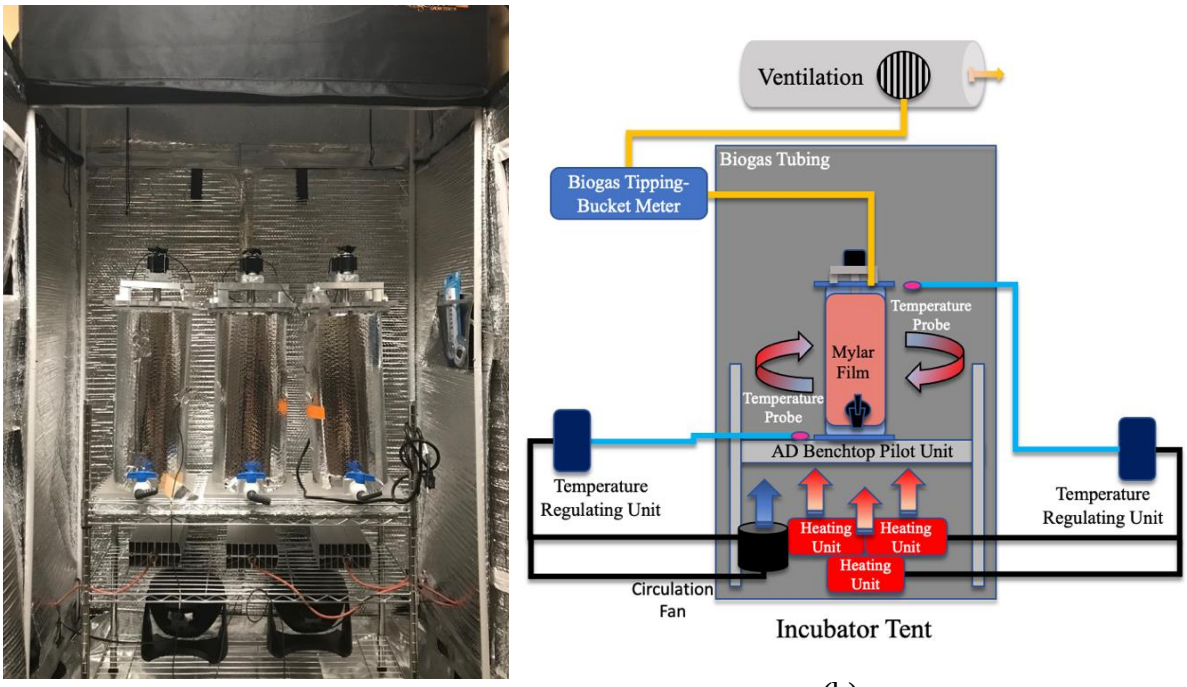

(a) (b)

Figure 6. Pilot-scale AD tent system setup: (a) The mechanically mixed anaerobic digesters housed in an insulated tent; (b) The tent system configuration.

2.2.3 Chemical analysis

Chemical analyses and frequencies are summarized in Table 1. The concentrations of chemical oxygen demand (COD), total Kjeldahl nitrogen (TKN), total ammonia nitrogen (TAN), total phosphorus (TP), and Ortho phosphorus (OP) were measured using the Hach test kits of TNT 822, TNT 880, TNT 832, and TNT 845, respectively. Besides, protein nitrogen concentration was calculated as the difference between TKN and TAN. Dissolved organic nitrogen (DON) concentration was calculated as the difference between soluble TKN (sTKN) and TAN. Free ammonia nitrogen (FAN) was calculated based on the chemical equilibrium between unionized ammonia and ammonium ion. Dissolved organic phosphorus (DOP) was calculated as the difference between total soluble phosphorus (sTP) and OP. Moreover, pH, alkalinity, and volatile fatty acids (VFA) were measured with a HANNA HI901C Automatic Potentiometric Titrator. TS, volatile solids (VS), suspended solids (SS), and volatile suspended solids (VSS) were measured according to the standard methods (APHA, 2012).

Particle size distribution and viscosity tests were conducted using a particle analyzer (LA-950, Horiba, CA, USA) and a viscosity meter (DV2T, AMETEK Brookfield, MA, USA), respectively. In order to evaluate the effects of THP and anaerobic digestion on sludge viscosity, the TS values of THP influent and effluent were adjusted to 9%, and the TS values of AD influent and effluent were adjusted to 5%, respectively. The dewaterability of THP influent, AD influent, and AD effluent was evaluated by the raw sample capillary suction time (CST) test using a capillary suction timer (294-50, Ofite, TX, USA). The volume expansion test of AD system was performed according to the method proposed by a previous work (Bartek et al., 2017). In short, the profiles of sludge volume expansion along with the time after feeding were obtained with and without mixing at the speed of 50 rpm.

Methane, hydrogen, and hydrogen sulfide contents in biogas were measured using a gas chromatography equipped with both a thermal conductivity detector and a flame photometric detector (GC-2014, Shimadzu, Columbia, MD). Ammonia content in biogas was calculated based on Henry's law. The biogas production rate was real-time monitored using calibrated tipping-bucket meters coupled with automatic data loggers (Archae Press, Nashville, USA). A summary of these and other biogas analysis parameters can be found in Table 2. Additionally, biogas samples from three AD systems during steady state were collected using the Summa canisters and Tedlar air sampling bags and shipped to the external lab (ALS global, CA, USA) for total sulfur and siloxane analysis. The dewatered AD effluent cake samples were sent to another external lab (Huffman Hazen Laboratories, CO, USA) for British thermal unit (BTU), carbon, hydrogen, nitrogen, and sulfur (CHNS) analysis. The metal contents were analyzed with an Inductively Coupled Plasma (ICP). EPA Part 503 metals including arsenic, cadmium, copper, lead, mercury, molybdenum, nickel, selenium, and zinc were also analyzed with ICP. All the parameters measured multiple times as indicated in Tables 1 and 2 are presented as the mean values with the standard errors.

Table 1. Summary of chemical analysis

Parameters	THP Feed	AD Influent	AD Effluent	Filtrate	Cake	Frequency
TS, VS	X	X	X	X	X	Weekly for THP and AD

SS, VSS					X	Weekly at steady state
tCOD	X	X	X	X		Weekly at steady state
sCOD, <1.5 µm		X	X	X		Weekly at steady state
sCOD, <0.45 µm		X	X	X		Weekly at steady state
TKN	X	X		X		Weekly at steady state
sTKN <0.45 µm		X	X	X		Weekly at steady state
NH_4^+	X	X	X	X		Weekly at steady state
TP	X	X	X	X		Weekly at steady state
sTP, PO_4^{3-} (<0.45 µm)		X	X	X		Weekly at steady state
VFA		X	X	X		Every other day
pH, alkalinity			X	X		Every other day
Ca, Mg, Na, K, Fe, Al	X	X	X			Three times at steady state
Biogas production rate			X			Real-time
Methane content			X			Weekly
Viscosity	X	X	X			Once at steady state
Rapid volume expansion			X			Three times at steady state
BTU Content					X	At steady state/end
503 Metals					X	At steady state/end
CHNS					X	At steady state/end
CST	X	X	X			At steady state/end

Table 2. Biogas monitoring parameters and frequency

Parameters	Digester Gas	Frequency

Production Rate	X	Daily
Biogas Yield	X	Weekly
Methane Yield	X	Weekly
Methane (CH_4)	X	Weekly
Hydrogen (H_2)	X	Steady state
Hydrogen Sulfide	X	Steady state
Total Sulfur	X	end
Ammonia	X	Steady state
Siloxanes	X	end

2.3 Dewatering test

The digester effluent dewatering test was conducted at Bucknell University using the optimized centrifuged methods proposed in Dr. Higgins's previous work (Higgins et al., 2014) (Table 3). The AD systems were sacrificed in the morning of the day, and the AD effluent samples were driven to Bucknell's lab for the dewatering test on the same day. The polymer selected for the dewatering test was Flopam Fo 4440, and the CST tests were performed prior to dewatering in order to determine the optimal polymer dose (OPD) for each sample prior to dewatering. The TS and VS of each dewatered cake sample were measured according to the standard method (APHA, 2012). In order to verify the approach of the lab-scale dewatering test, two rounds of dewatering verification tests were conducted in both Bucknell lab and VT lab using centrifuge and piston methods, respectively. The details of the piston method can be found in our previous published work (Luo et al., 2021). The details of the two rounds of verification test design are summarized in Table 4 (a) and 4 (b).

Table 3. Pilot AD effluent dewatering approach

Group	Sample	Polymer	TS	CST	Method
Arlington 10-day	Pilot THP-AD effluent	Bucknell (Fo 4440)	√	√	Bucknell method

Arlington 12.5-day	Pilot THP-AD effluent	Bucknell (Fo 4440)	√	√	Bucknell method
Arlington 15-day	Pilot THP-AD effluent	Bucknell (Fo 4440)	√	√	Bucknell method

Table 4 (a). 1st round verification of dewatering approach

Group	Sample	Polymer	TS	CST	Method
DC water-Bucknell polymer	DC Water digestate	Bucknell (Fo 4440)	√	√	Bucknell method
Arlington-Arlington polymer (plant dose)	Arlington raw thickened sludge	Arlington	√		Bucknell method
Arlington-Arlington polymer	Arlington raw thickened sludge	Arlington	√	√	Bucknell method
Arlington-Bucknell polymer	Arlington raw thickened sludge	Arlington	√	√	Bucknell method

Table 3 (b). 2nd round verification of dewatering approach

Group	Sample	Polymer	TS	CST	Method
Bucknell-Arlington polymer	Arlington raw thickened sludge	Arlington	√	√	Bucknell method
Bucknell-Bucknell polymer	Arlington raw thickened sludge	Bucknell (Fo 4440)	√	√	Bucknell method
VT-Arlington polymer	Arlington raw thickened sludge	Arlington	√	√	VT method
VT-Cake	Arlington raw cake		√		Oven (Bucknell)
Bucknell-Cake	Arlington raw cake		√		Oven (VT)

3 Results and Discussions

3.1 AD startup and steady state

All three ADs were fed with the THP-AD seed collected from DC Water. As shown in Figure 7a, the SRTs of three ADs were all operated at 30 days on Day 1 (6/4/2021) and then dropped by 0.5d

per day until they reached 16d at which the SRTs of all three ADs were upheld for 1.5 months until the end of July (60 days) for the high VFA measured in the system (Figure 7b). After that, the SRT of three ADs were further reduced to 15d on Day 69 (8/11/2022) and upheld there for another 1.5 months. Then, the SRTs of two out of the three ADs were further dropped at a pace of 0.5d every other day until they reached 12.5d and 10d, respectively. On Day 120 (10/1/2022), the last AD reached a 10 d SRT.

During the startup operation, pH, VFA, and alkalinity were monitored three to four times a week. As shown in Figure 7c, the pH dropped from 8 to 7.6 during the first two weeks following the seeding until Day 14 (6/17/2022). Then pH was stabilized between 7.5 to 7.7 in all three ADs. Usually, VFA and alkalinity concentrations can be used as indicators of the system condition. As shown in Figure 7b and 7d, both VFA and alkalinity dropped along with the decrease of SRTs. However, the VFA/alkalinity ratio increased from 0.3 to 0.5 during the startup (Figure 7e). According to our previous study (Zhang et al., 2020), a VFA/alkalinity ratio below 0.5 is acceptable for the stable operation of ADs fed with THP sludge, even though the conventional AD fed without THP sludge was usually expected to be operated at a VFA/alkalinity ratio below 0.4. It should be noted that the abnormal increase of VFA/alkalinity ratios at the end of November (day 170) was very likely due to the plant operation mode switching from summer to winter modes, i.e., the SRT of biological treatment process is higher in the winter than in the summer. (Figure 7e).

After all ADs had been operated for 190 days, T-test was performed to assess whether statistical difference can be found in the daily biogas production rates over the past three SRTs as a means to confirm steady states have been reached (Figure 7f). According to the T-test, all three ADs had reached steady state on Day 190 (12/10/2021). Thereafter, four rounds of steady-state chemical analyses were conducted until Day 218 (1/7/2022). The abnormal values of biogas production rates measured in September were due to the tipping bucket problems which were fixed at the beginning of October (Figure 7f).

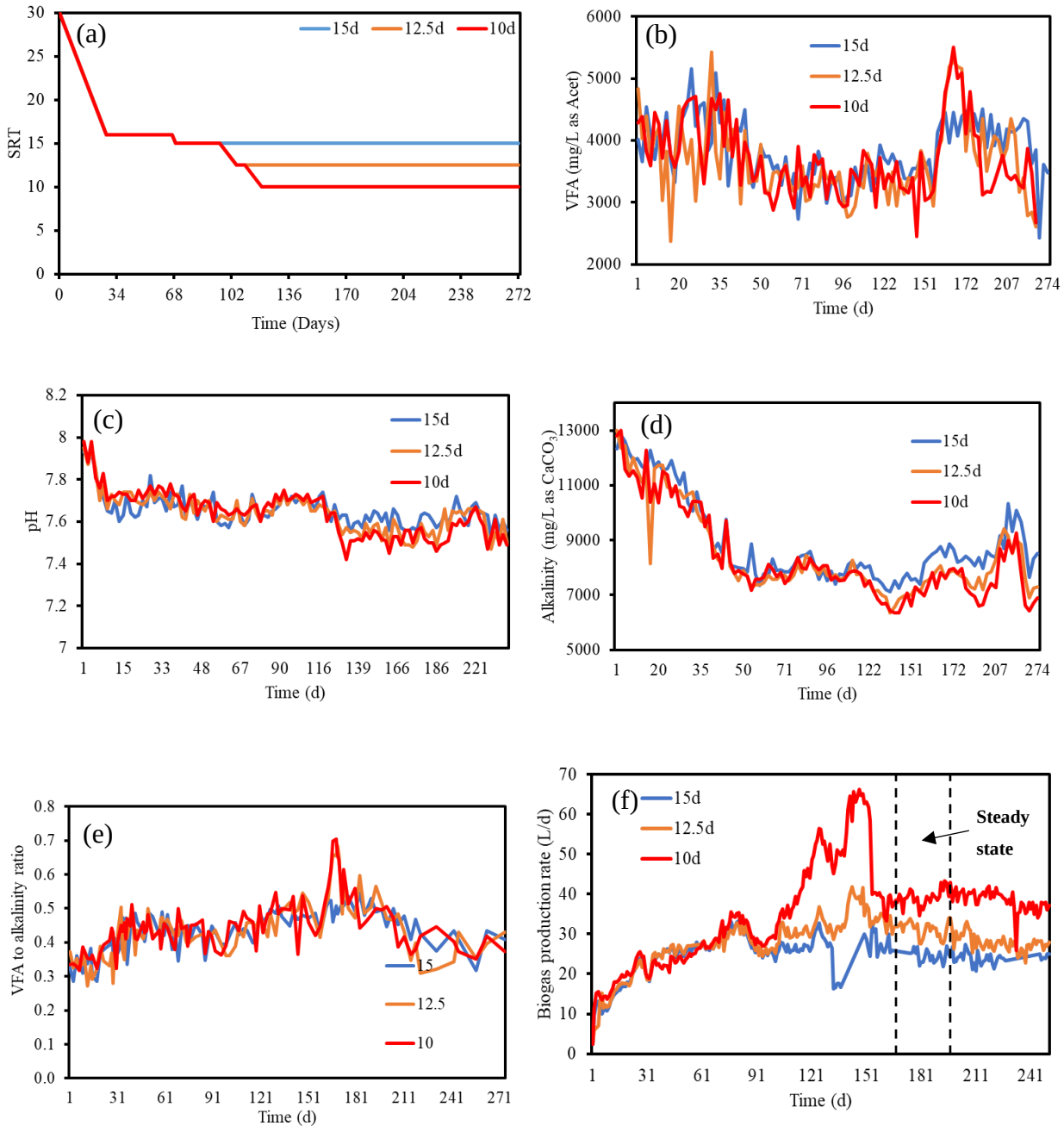

Figure 7. (a) SRT, (b) VFA, (c) pH, (d) alkalinity, (e) VFA/alkalinity ratio, and (f) biogas production rate profiles during the startup and steady states of the three ADs

During the startup and steady-state operation, the AD effluent soluble COD (sCOD), TAN, FAN, total solids reduction (TSR), volatile solids reduction (TSR), and biogas CH_4 content were also

monitored on a weekly basis. As shown in Figure 8a and 8b, both TAN and FAN decreased over the entire project duration, especially during the startup when SRTs were reduced. In contrast, effluent sCOD fluctuated between 4,000 and 6,000 mg/L until the end of November and then gradually climbed up to around 9,000 mg/L throughout the rest of the project phase in all three ADs (Figure 8c), probably due to the seasonal operation mode change in AWPCP.

TSR and VSR of three ADs were similar during the first four months when the same SRTs were used in all ADs (Figure 8 d and e). After SRTs in two ADs were further reduced in October, their TSR and VSR values became smaller and appeared to be in a positive correlation with the SRT values used in each AD (Figure 8 d and e). Again, abnormal fluctuations in sCOD, TSR, and VSR showed up in December 2021 along with the VFA and alkalinity fluctuation. Interestingly, the biogas CH_4 content remained stable around 60% throughout the project duration, indicating the methanogen inhibition problem has not been encountered in this project (Figure 8f).

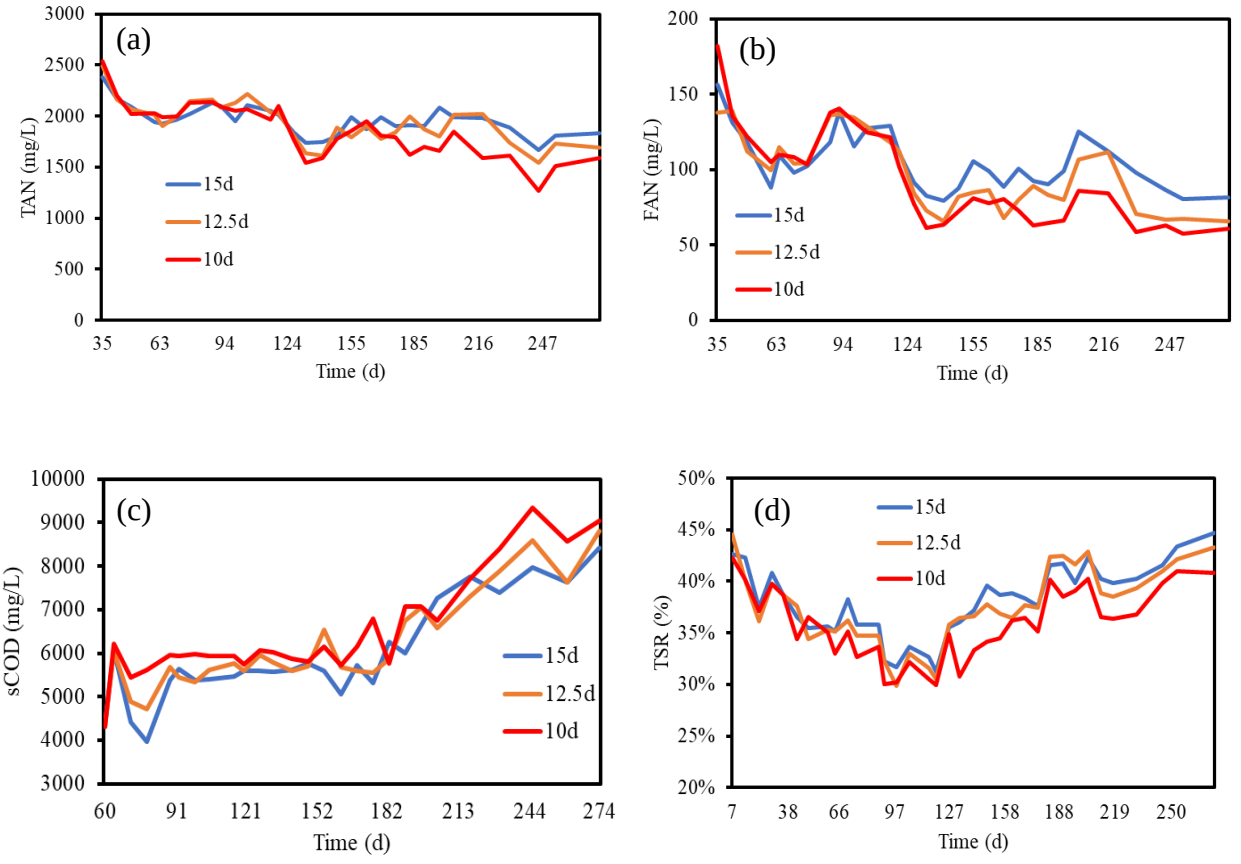

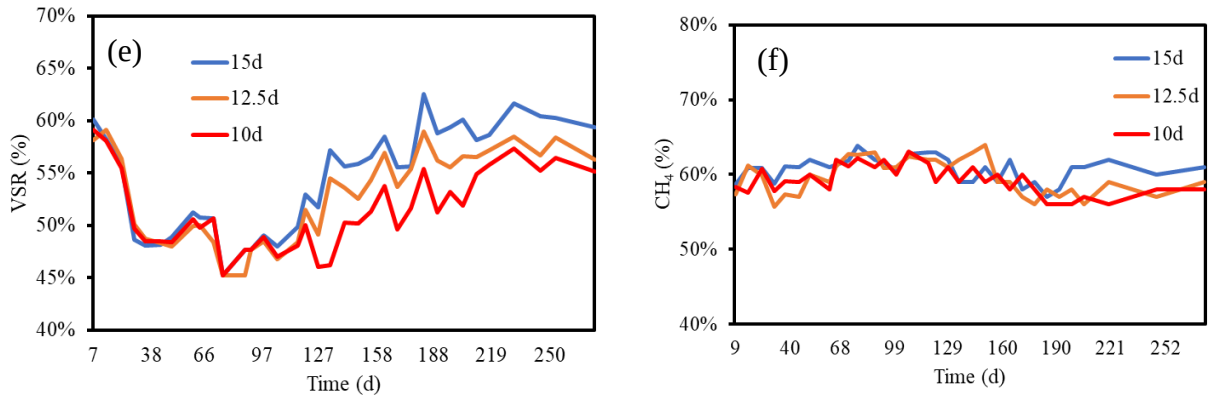

Figure 8. (a) TAN, (b) FAN, (c) sCOD, (d) TSR, (e) VSR, and (f) CH_4 content profiles during the startup and steady state of all three ADs

3.2 Steady-state chemical analysis

3.2.1 TSR, VSR, and methane yield

As shown in Figure 9, when all ADs reached steady state, VSR and TSR were positively related to the SRTs, which is expected because a longer SRT allows a more complete digestion (Figure 9 a and b). However, VSR and TSR only dropped 7.08 ± 0.006% and 3 ± 0.008% when the SRT dropped from 15d to 10d, indicating that a lower SRT may has less impact on the organics removal of the sludge pretreated with THP. Likewise, the methane yield was slightly lower (e.g., 6.9 ± 0.08%) in ADs operated at 12.5d and 10d SRTs than the AD at 15 days (Figure 9c). Therefore, it can be concluded that lowering SRT from 15d to 10d can slightly reduce methane productivity.

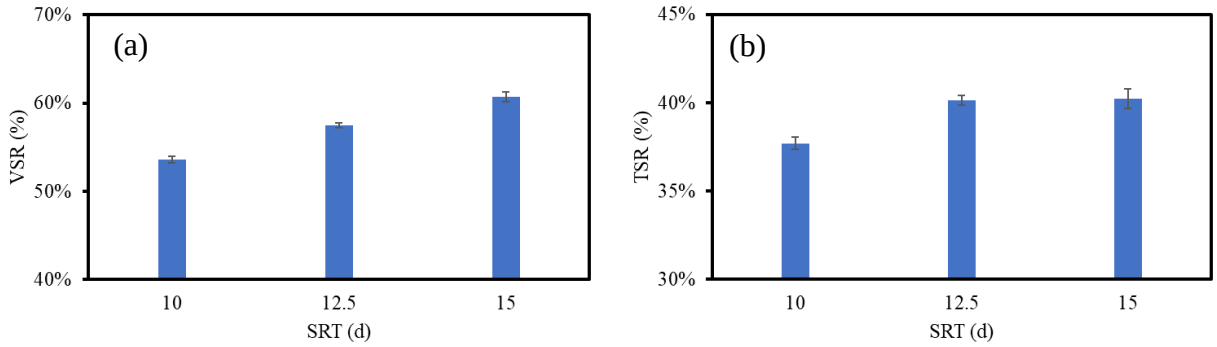

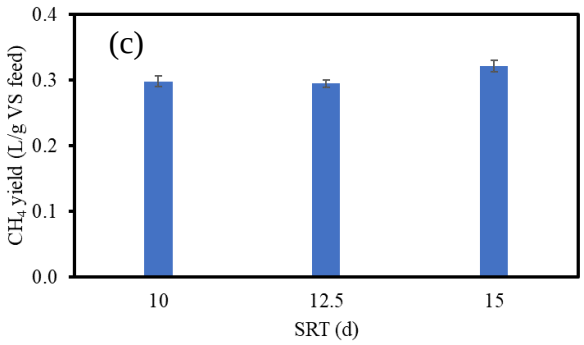

Figure 9. Steady-state (a) VSR, (b) TSR, and (c) CH_4 yield of ADs operated at different SRTs

3.2.2 COD and Nitrogen

Total COD (tCOD), sCOD, TKN, sTKN, TAN, protein nitrogen, and DON of THP influent, AD influent, and AD effluent were measured four times on a weekly basis at the steady state. Results in Figure 10a show that it was the anaerobic digestion but not the THP that has reduced the tCOD, which is reasonable because methane is the only COD that can leave the system. Again, tCOD in AD effluent was inversely related to the SRT based on the time allowable for organic removal. In contrast, TKN consisting of both protein and ammonia nitrogen remained unchanged during both THP and anaerobic digestion processes because very little nitrogen can leave the system (Figure 10b). Soluble components of the AD influent included 25,000 mg/L sCOD, 2,200 mg/L sTKN, 500 mg/L TAN, and 1,800 mg/L DON as a result of the thermal hydrolysis (Figure 10 c, d, e, and f). Similar to tCOD, the AD effluent sCOD was inversely related to SRT based on the time allowable for sCOD utilization (Figure 10c). However, AD effluent sTKN was positively related to SRT as shown in Figure 10d. This is because TAN is the final product of protein degradation as shown in Figure 10g. However, no correlation was found between DON and SRT, indicating the remaining DON might be non-readily biodegradable in ADs (Figure 10f). Because protein is usually degraded after carbohydrates (Yang et al., 2015), the similar DON concentration in AD effluent with three different SRTs suggests rather complete anaerobic digestion efficiencies even at SRTs of 10 and 12.5 days as shown in Figure 9 a and b.

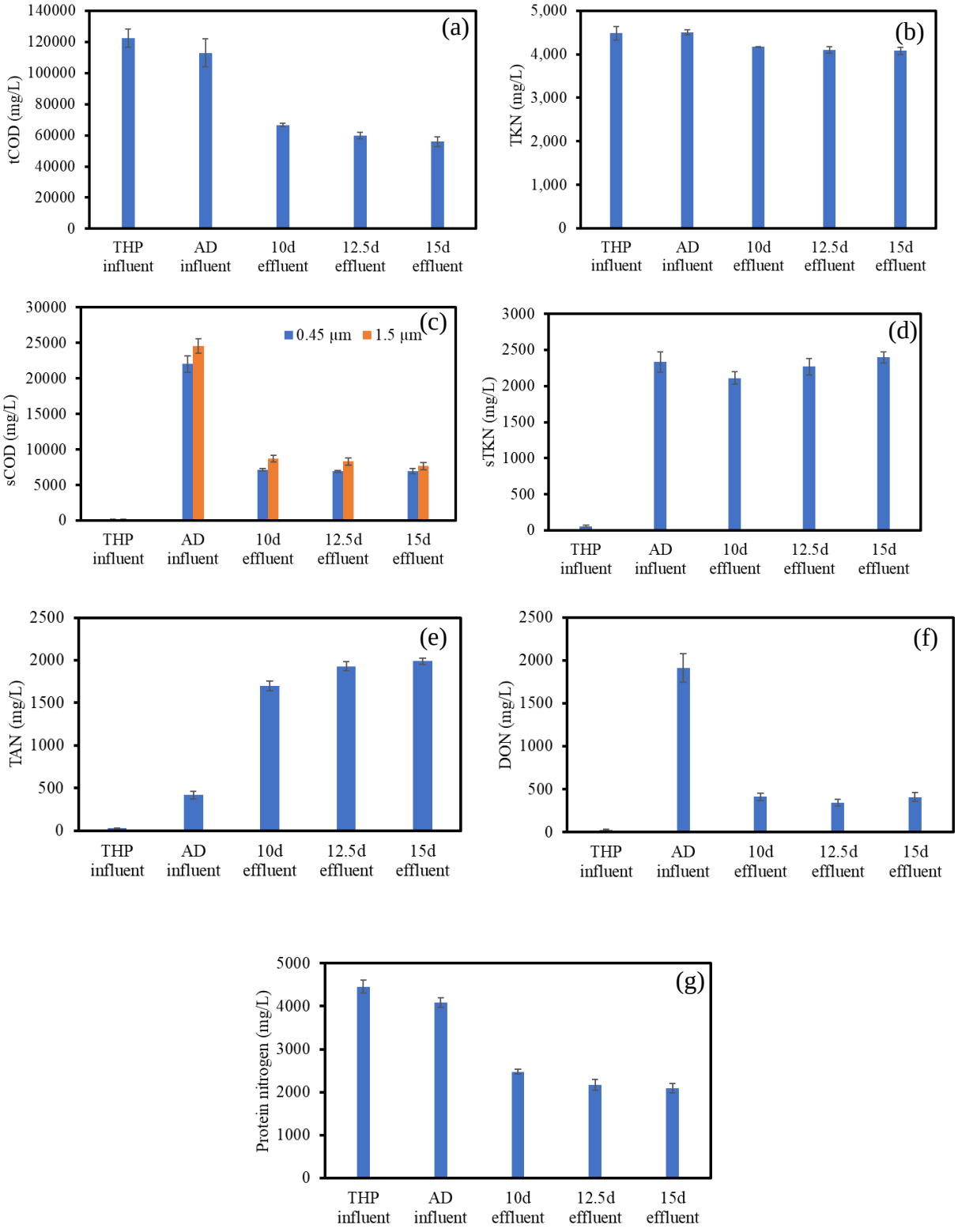

Figure 10. Steady-state (a) tCOD, (b) TKN, (c) sCOD, (d) sTKN, (e) TAN, (f) DON, and (g) protein nitrogen concentrations of THP influent, AD influent and AD effluent at different SRTs

3.2.3 Phosphorus

TP and sTP including DOP and OP in THP influent, AD influent, and AD effluent were also measured four times on a weekly basis (Figure 11). As can be seen, TP almost remained unchanged after THP and decreased around 10% after anaerobic digestion (Figure 11 a). At this moment, we do not understand why TP decreased after anaerobic digestion. The only hypothesis we have is that insoluble P precipitation might have been deposited on the AD inner walls. In contrast, substantial amounts of soluble P have been released in THP, i.e., 150 mg/L sTP including 40% OP and 60% DOP (Figure 11 b, c, and d). No relationship was observed between SRT and OP or DOP.

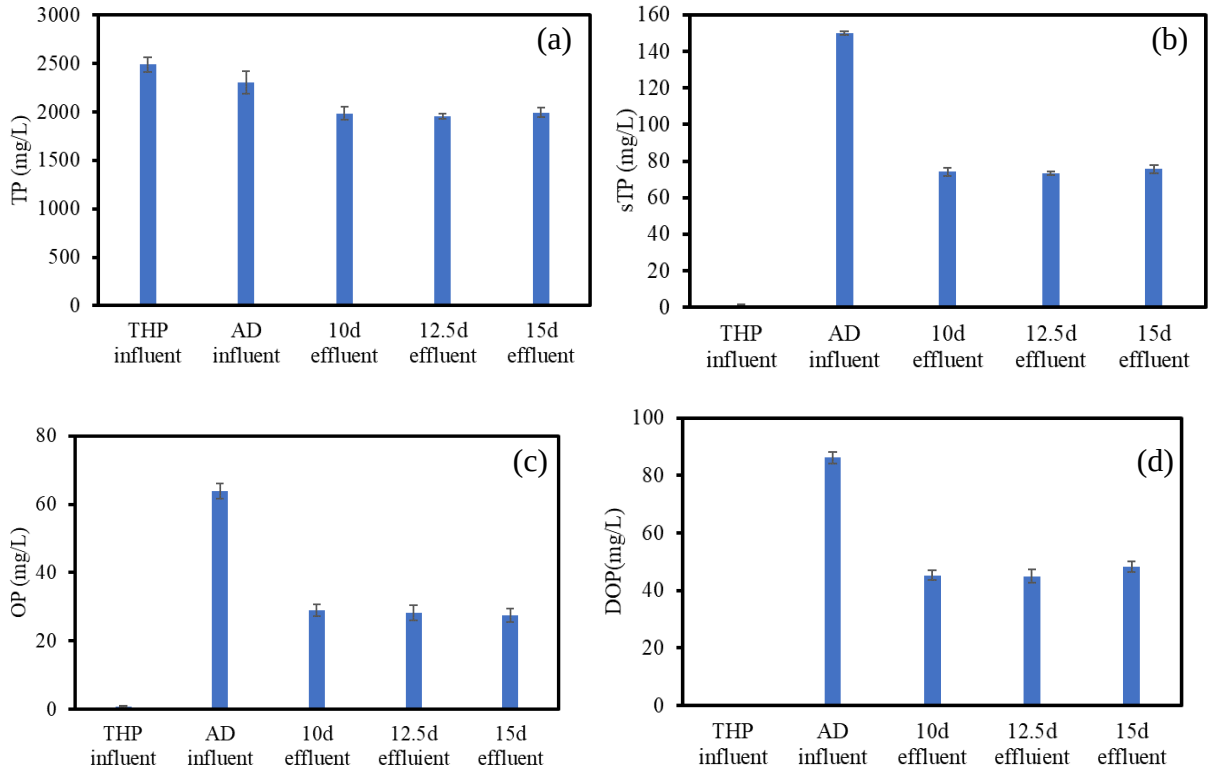

Figure 11. Steady state (a) TP, (b) sTP, (c) OP, and (d) DOP concentrations in THP influent, AD influent, and AD effluent at different SRTs

3.2.4 Metals

Total and soluble Na, Mg, Ca, Al, K, and Fe concentrations of THP influent, AD influent, and AD effluent were also measured during the steady state. As shown in Figure 12, total Na, Mg, Ca, Al, K, and Fe concentrations calculated on the ash mass basis almost remained unchanged after THP

and anaerobic digestion, as expected. Soluble metals in Figure 13 increased in ADs as a result of organics degradation, with the exception of Mg and Fe. The formation of struvite ($NH_4MgPO_4 \cdot 6H_2O$) might explain the soluble Mg reduction (Figure 13b) and the TP reduction (Figure 11a). The FeS formation from H_2S and Fe^{2+} may explain the soluble Fe reduction (Figure 13f) as reported by (Luo et al., 2022). Most soluble metal concentrations were inversely related to SRTs, indicating more complete anaerobic digestion might have resulted in more metal precipitation (Figure 13). It is also noteworthy that Fe was significantly more abundant than other metals because ferric polymer has been used in AWPCP as a coagulant.

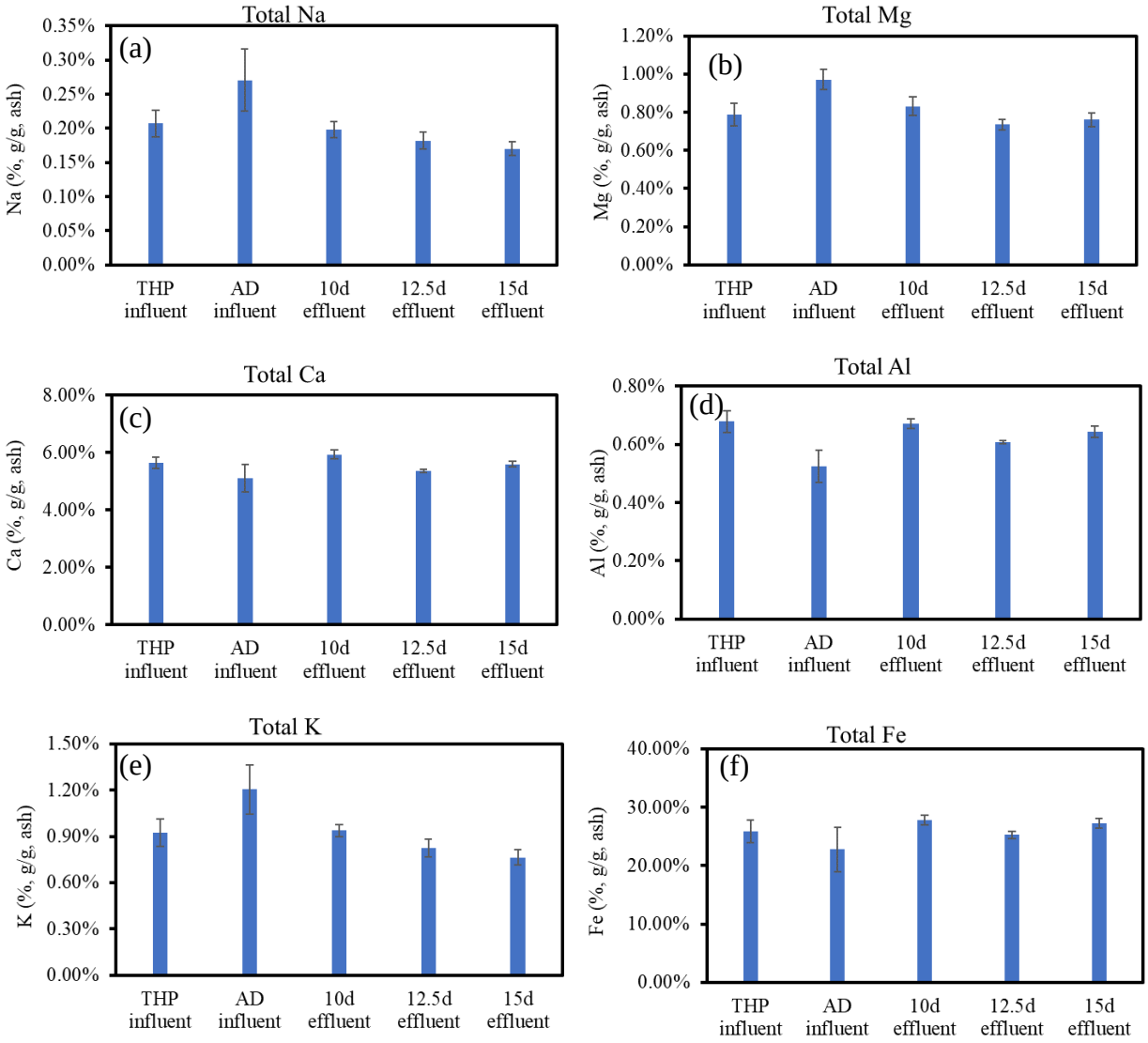

Figure 12. Steady state total (a) Na, (b) Mg, (c) Ca, (d) Al, (e) K, and (f) Fe concentrations of THP influent, AD influent, and AD effluent at different SRTs

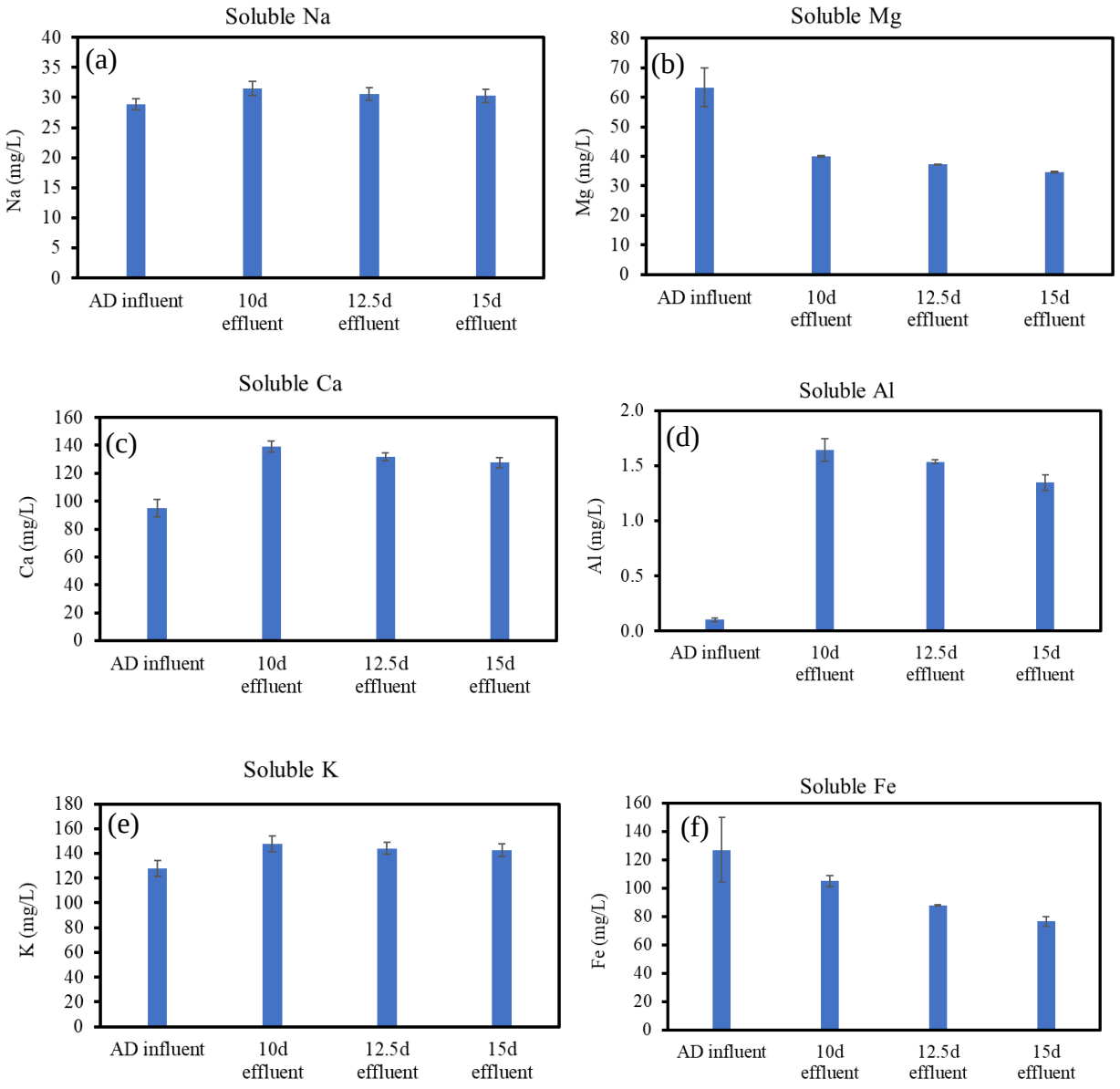

Figure 13. Steady state soluble (a) Na, (b) Mg, (c) Ca, (d) Al, (e) K, and (f) Fe concentrations of AD influent, and AD effluent at different SRTs

3.2.5 Particle size, viscosity, CST, and rapid volume expansion

As shown in Figure 14, sludge particle size was reduced after THP and was further reduced after anaerobic digestion as a result of both thermal hydrolysis and biological degradation. However,

no correlation was observed between SRTs and particle sizes, which again indicates rather complete anaerobic digestion has been achieved with all SRTs, resulting in similar TSR in all three ADs (Figure 9b). The viscosity of sludge decreased after THP and further decreased after anaerobic digestion (Figure 15), which exhibited a similar trend as that of the particle size. Again, no relationship was observed between SRT and viscosity (Figure 15b). Moreover, CST of all sludge samples were also measured, and a larger CST value indicates the poorer dewaterability. Therefore, CST results in Figure 16 showed that the sludge dewaterability actually decreased after THP, which contradicts the conventional understanding that THP can improve the sludge dewaterability. For example, previous study indicated THP reduced CST from 110.4 s to 29.6s (Zhang et al., 2021b; Shi et al., 2021; Bougrier et al., 2008). Furthermore, sludge CST value increased around fivefold after anaerobic digestion, indicating the even worse dewaterability of the sludge after anaerobic digestion which is expected (Novak et al., 2003). The rapid volume expansion test was conducted with mixing and without mixing for each reactor SRT based upon the agreement of the team. For each reactor either with or without mixing, the sludge volume level in the reactor was recorded every 10 minutes until it reached a plateau after sludge feeding. Figure 17 shows that mechanical mixing can reduce the volume expansion from 8-15% to around 2%, indicating the essential role of mechanical mixing in reducing the foaming during anaerobic digestion. In addition, lower SRTs showed higher expanded volumes probably as a result of the higher organic loading rates.

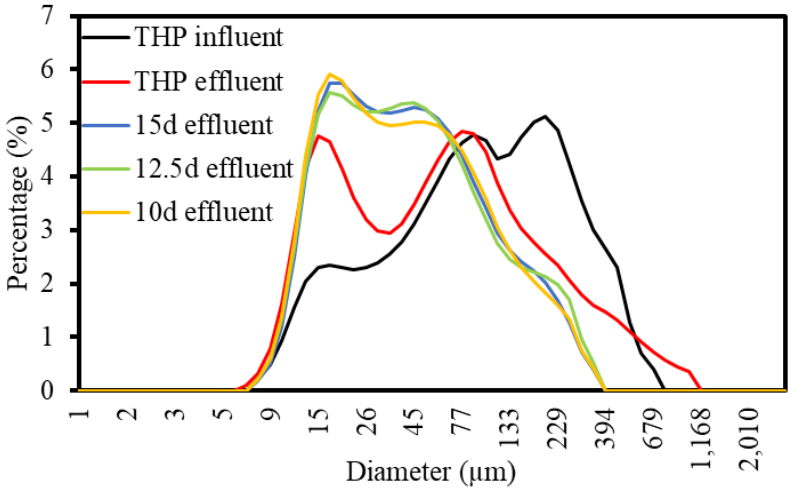

Figure 14. Particle size distribution of THP influent, AD influent, and AD effluent at different SRTs

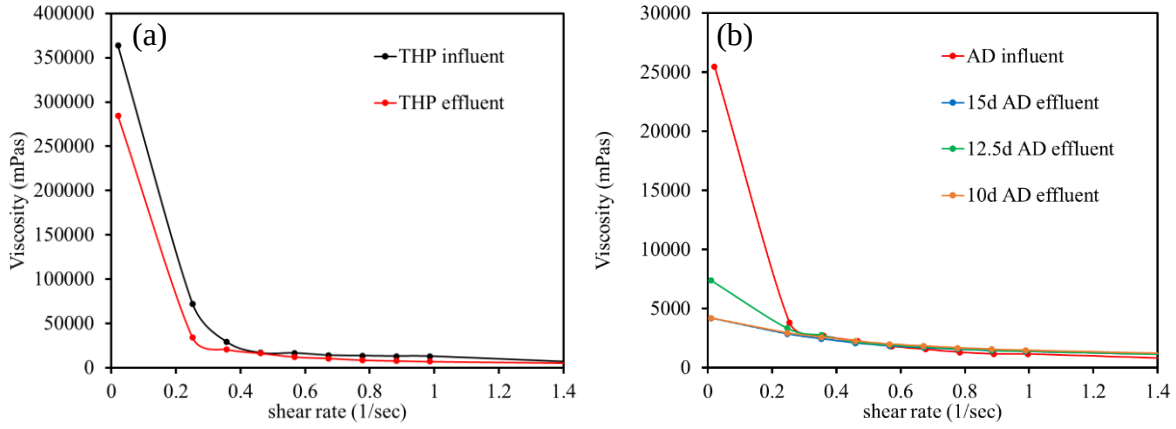

Figure 15. Viscosity of sludge (a) before and after THP and (b) before and AD at different SRTs

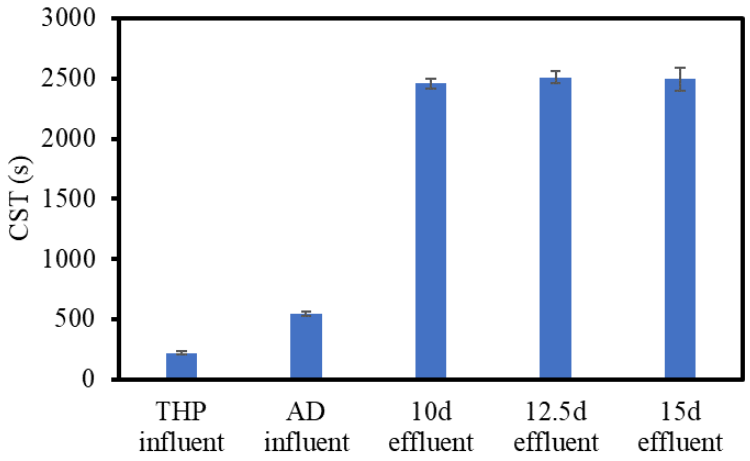

Figure 16. CST of THP influent, THP effluent, and AD effluent

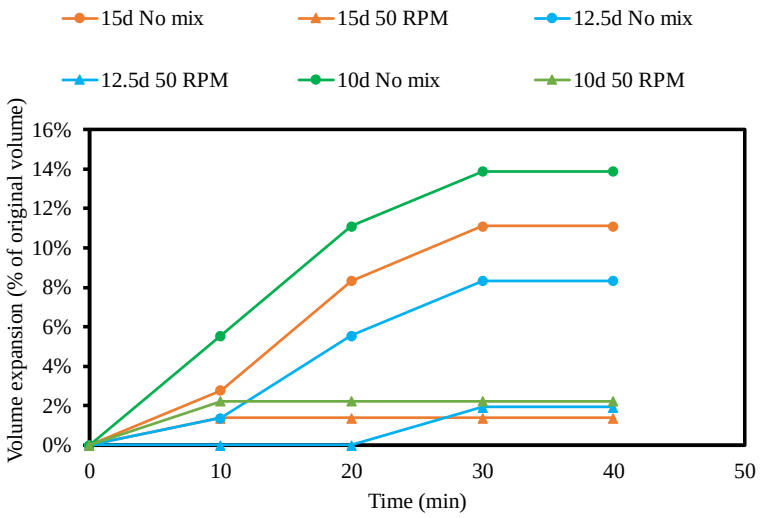

Figure 17. Steady state ADs volume increased over time during the rapid volume expansion tests with and without physical mixing at different SRTs

3.2.6 Biogas composition

Figure 18 shows the NH_3, H_2S, H_2, and CH_4 content in the biogas. In short, all except CH_4 were below 1% and did not show any dependence on the AD SRT. A further look into the sulfur compound compositions in Table 5 shows that majority of the sulfur compounds were at nondetectable levels in biogas. However, the total sulfur concentration from AD operated at 15d SRT was significantly lower than those ADs operated at 10d and 12.5d SRT. This may be explained by their precipitation with soluble Fe which shared a similar trend in Figure 13f. This phenomenon has been summarized in previous work (Luo et al., 2022). Table 6 shows the siloxane composition. Biogas typically contains a small percentage of siloxane which has strong adverse effects on the utilization of biogas. The combustion of biogas containing siloxane will produce microcrystalline silica which can cause damage to generators, turbines, and fuel cells (Ruiling et al., 2017). Again, the majority of the siloxane species cannot be detected. The total siloxane concertation in biogas was below 2 mg/m^3, which means biogas siloxane concentration in this study was lower than the commonly required concentration limit (15 mg/m^3) of engine manufacturers (Ruiling et al., 2017).

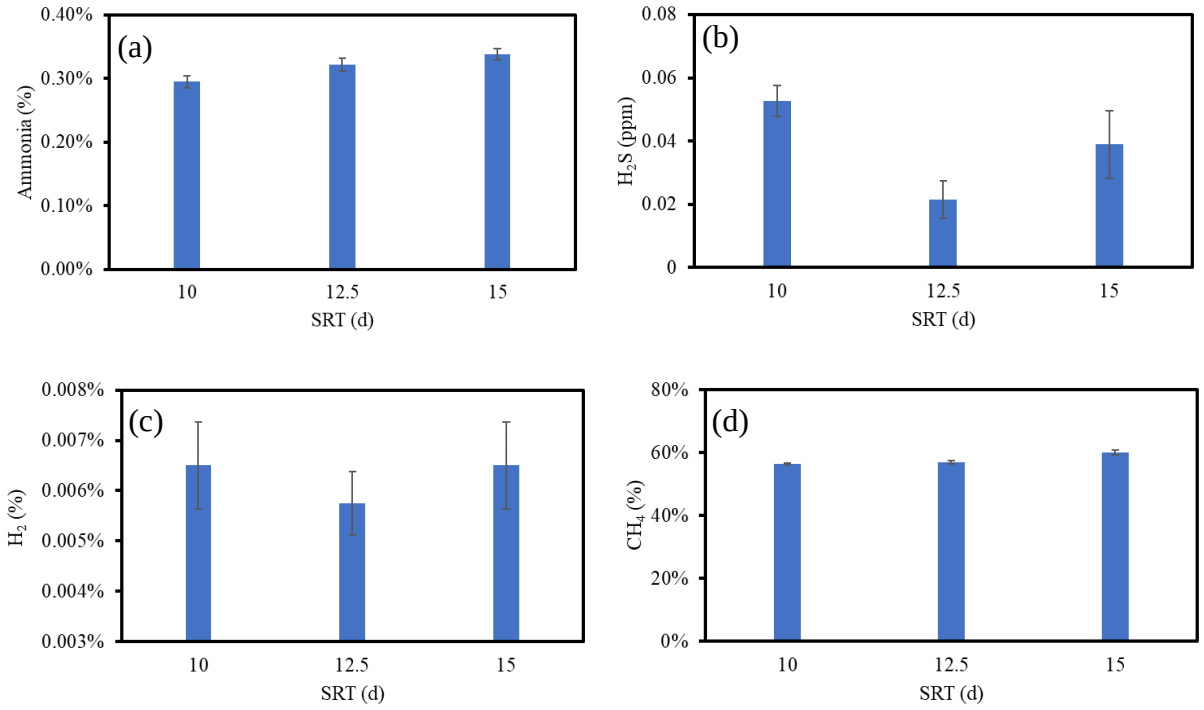

Figure 18. Steady state (a) ammonia, (b) H_2S, (c) H_2, and (d) CH_4 concentrations in the biogas of AD system at different SRTs

Table 4. Summary of the sulfur composition in biogas during steady state of AD

Compounds	Results (µg/m^3)			*MRL (µg/m^3)
	15d	**12.5d**	**10d**	
Hydrogen Sulfide	97	*ND	ND	15
Carbonyl Sulfide	ND	76	86	27
Methyl Mercaptan	ND	ND	ND	22
Ethyl Mercaptan	ND	ND	ND	28
Dimethyl Sulfide	ND	72	57	28
Carbon Disulfide	ND	21	21	17
Isopropyl Mercaptan	48	ND	ND	34
tert-Butyl Mercaptan	ND	ND	ND	41
n-Propyl Mercaptan	ND	ND	ND	34
Ethyl Methyl Sulfide	ND	ND	ND	34
Thiophene	ND	100	91	38
Isobutyl Mercaptan	ND	67	70	41
Diethyl Sulfide	ND	ND	ND	41

n-Butyl Mercaptan	ND	ND	ND	41
Dimethyl Disulfide	ND	33	33	21
3-Methylthiophene	ND	48	ND	44
Tetrahydrothiophene	ND	ND	ND	40
2,5-Dimethylthiophene	ND	ND	ND	50
2-Ethylthiophene	ND	ND	ND	50
Diethyl Disulfide	ND	ND	ND	27
Total reduced sulfur as H_2S	150	820	630	

Table 5. Summary of siloxane composition in biogas during steady state of AD

Compounds	**Results as Silicon ($\mu g/m^3$)**			**MRL ($\mu g/m^3$)**
	15d	**12.5d**	**10d**	
Trimethylsilanol	ND	ND	ND	270
Hexamethyldisiloxane (L2)	ND	ND	ND	300
Hexamethylcyclotrisiloxane (D3)	ND	ND	ND	380
Octamethyltrisiloxane (L3)	ND	ND	ND	310
Octamethylcyclotetrasiloxane (D4)	280	ND	ND	330
Decamethyltetrasiloxane (L4)	ND	ND	ND	320
Decamethylcyclopentasiloxane (D5)	1800	1700	1200	330
Dodecamethylpentasiloxane (L5)	ND	ND	ND	320
Dodecamethylcyclohexasiloxane (D6)	ND	ND	ND	330
Total Silicon	2080	1700	1200	

- *ND = Compound was analyzed for, but not detected above the laboratory reporting limit. *MRL = Method Reporting Limit - The minimum quantity of a target analyte that can be confidently determined by the referenced method.

3.3 Dewatering test

3.3.1 Polymer dose

The OPD was determined based on the CST test result as shown in Figure 19, i.e., 36.6, 37, and 46 lb/ton for sludge produced from ADs operated at 10d, 12.5d, and 15d SRTs. It can be seen that OPD increased with the increase of SRT. A longer SRT usually grows greater concentration of bacterial cells and EPS, which demand more polymer for dewatering (Luo et al., 2022).

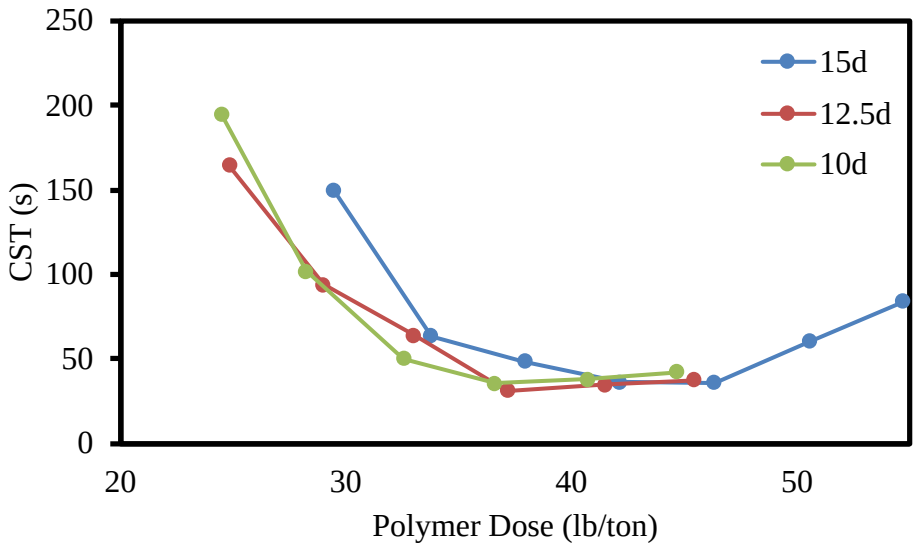

Figure 19. CST of AD effluent at various polymer doses

3.3.2 Dewatered cake dryness

As shown in Figure 20, the cake dryness in terms of TS were 19.8%, 20.4%, and 17.8% for the ADs effluent operated at SRT of 10d, 12.5d, and 15d. According to the methodology of the lab-scale dewatering test at Bucknell, around 4-5 % TS need to be added to the final TS results in order to predict the TS that will be obtained in the full-scale centrifuge dewatering system. Therefore, the dewatered cake TS should be extrapolated to 24.8%, 25.4%, and 22.8% for all three ADs at the full-scale application in AWPCP. Still this result is much lower than typically expected for THP AD sludge (~30%).

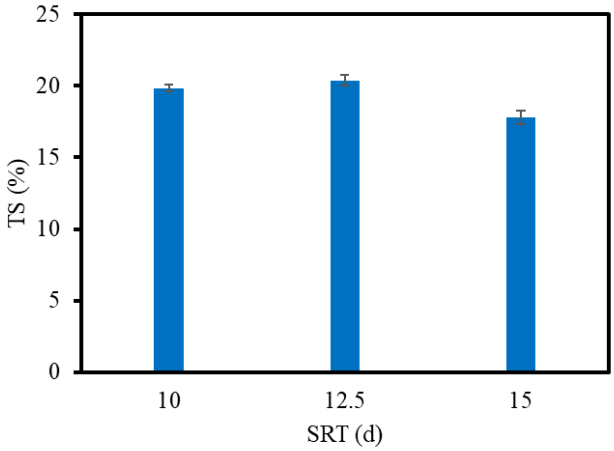

Figure 20. TS of dewatered cake at different SRTs

3.3.3 Lab-scale dewatering approach verification test

In order to verify the lab-scale dewatering reliability, two rounds of dewatering verification tests were separately conducted in Bucknell lab and VT lab using two different methods, namely the Bucknell method and VT method. Given that the influent characteristics of DC Water and AWACP are similar, DC Water also processes sludge through a THP system, and that both plants use ferric as coagulants during biological process, DC Water's AD effluent sludge was used as a benchmark for verifying the accuracy of the Bucknell method. Most importantly, Bucknell has done many studies related to the DC Water sludge dewaterability with sufficient database as a control. Detailed experimental design and terminology definition can be referred to Tables 4 a and b. As shown in Figure 21a, OPDs for DC Water AD effluent using Bucknell polymer, Arlington raw thickened sludge using Arlington polymer, and Arlington raw thickened sludge using Bucknell polymer were 30.78, 22.37, and 14.71 lb/ton, respectively.

Moreover, DC Water cake dryness was around 30% which is not far from DC Water full-scale results (Figure 21b). The Arlington sludge dewaterability measured by the Bucknell method with Arlington polymer and plant polymer dose, Arlington polymer and OPD, as well as Bucknell polymer and OPD showed very similar TS ranging from 21.25% to 22.7% (Figure 21b).

As can be seen in Figure 22a, the OPDs of Arlington sludge measured by Bucknell University and VT using Arlington polymer were very similar, i.e., 17.5 and 18.6 lb/ton, respectively, which is 30% lower than that measured using the Bucknell polymer (12.6 lb/ton).

The Arlington sludge dewaterability measured with Bucknell's lab-scale centrifuge method and VT's piston press method showed similar results in the TS ranging from 20 to 23% during 2nd round tests with the Arlington polymer, which is still around 5% lower than the TS of AWACP full-scale dewatered cake (Figure 22b). Hence, a 5% calibration adding to the lab dewatered cake TS results should be acceptable to predict the full-scale TS result.

It is noteworthy that there was almost no statistical difference between the cake dryness measured by VT and Bucknell on the same cake samples collected from AWACP (Figure 22b).

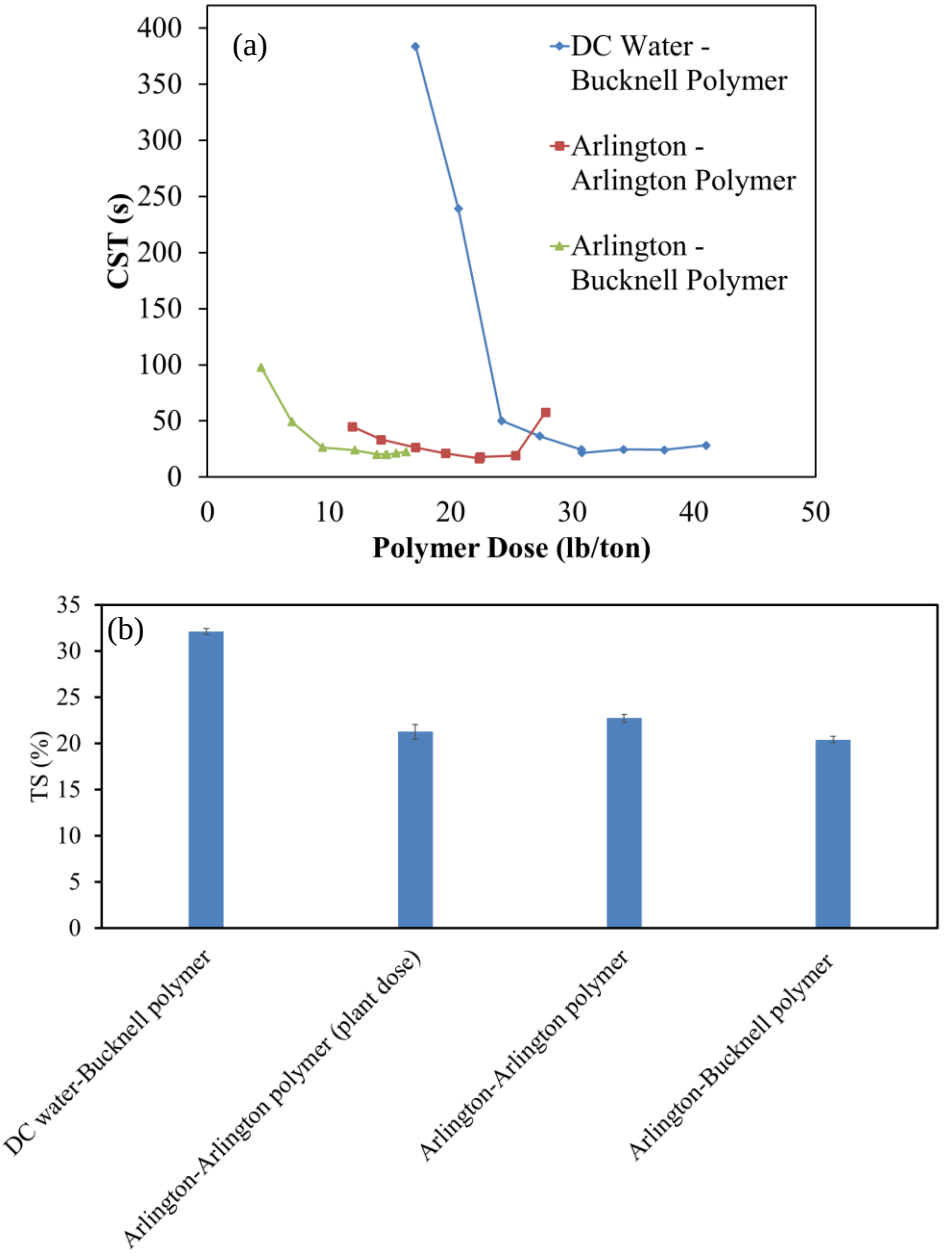

Figure 21. The 1st round verification of lab-scale dewatering approach: (a) CST of AWPCP full-scale centrifuge influent and DC Water AD effluent; (b) dewatered cake TS

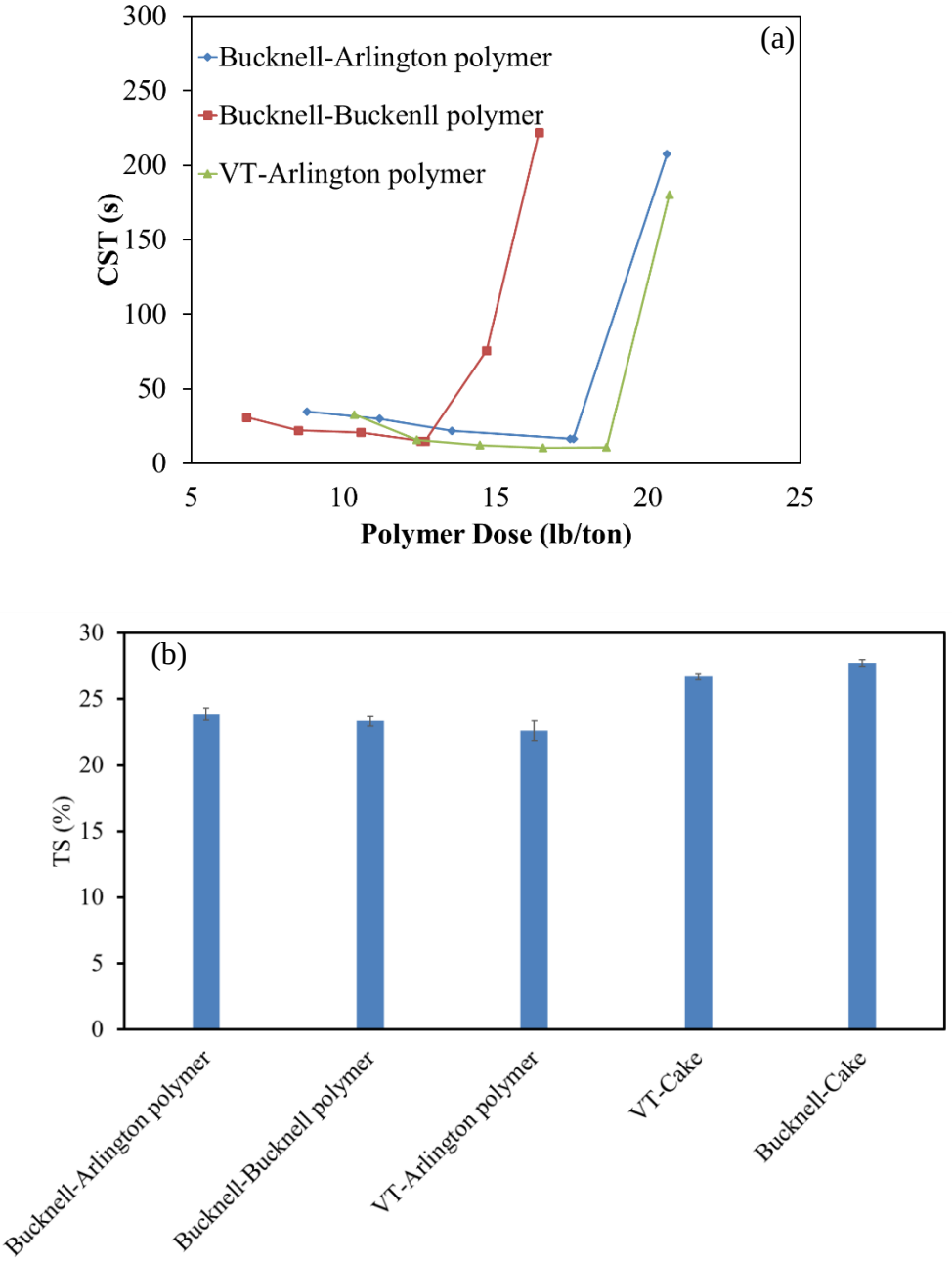

Figure 22. The 2nd round verification of lab-scale dewatering approach: (a) CST of AWPCP full-scale centrifuge influent; (b) dewatered cake TS

3.3.4 Dewatered cake elemental composition

As shown in Figure 23, most of the divalent and trivalent metal ions remained in the cake after dewatering, and almost half of the monovalent metal ions were released into the filtrate. This is reasonable because monovalent metal ions do not precipitate. The CHNS contents and BTU analysis results were also summarized in Table 7. It shows that a little bit more organics in terms of C, H, N, and BTU remained in sludge digested at shorter SRTs, respectively, which is in line with the TSR and VSR results in Figure 9 a and b. C/N·ash values has been used to predict dewatered cake dryness (Svennevik et al., 2019). WAS was usually considered to have poor dewaterability than PS as a result of higher viscosity and less free water than that of PS (Svennevik et al., 2019). C/N can be used as a substitute for the PS/WAS ratio since the C/N ratio of PS was found to be substantially higher than that of WAS as a result of higher protein fraction in WAS (Svennevik et al., 2019). Meanwhile, inorganic materials always have lower water capacity than organic materials (Miryahyaei et al., 2019). Additionally, inorganic compounds such as iron and aluminum compounds have also been shown to act as the skeleton builder in the sludge to improve sludge dewaterability (Luo et al., 2022). Therefore, both C/N and ash are positively related to sludge dewaterability, and combining the C/N ratio and ash content could be able to predict sludge dewaterability as reported in a previous published study (Svennevik et al., 2019). As shown in Figure 24, C/N·ash values of this study were 1.99, 2.06, and 2.15 for ADs operated at 10d, 12.5d, and 15d SRTs, respectively. Therefore, the TS contents predicted with equations in the study by Svennevik et al. (2019) are all below 25%, which is similar to the lab dewatering results (Figure 20). The ash contents (% TS) in this study were around 35% for all ADs which is in the range (36.7% to 41.6%) as indicated by previous studies (Liu et al., 2020; Jolis Domènec, 2008; Wang et al., 2018). Therefore, the lower C/N ratio in this study might be one of the reasons causing the poor dewaterability of the sludge in this study. Moreover, the EPA Part 503 metal concentrations of dewatered cake were summarized in Table 8. 503 metals are nine heavy metal pollutants commonly found in the biosolids including arsenic, cadmium, copper, lead, mercury, molybdenum, nickel, selenium, and zinc. The limited concentration for each of 503 metals is needed for land application (Management, 1994). All the 503 metal concentrations were lower than the limitations (Management, 1994).

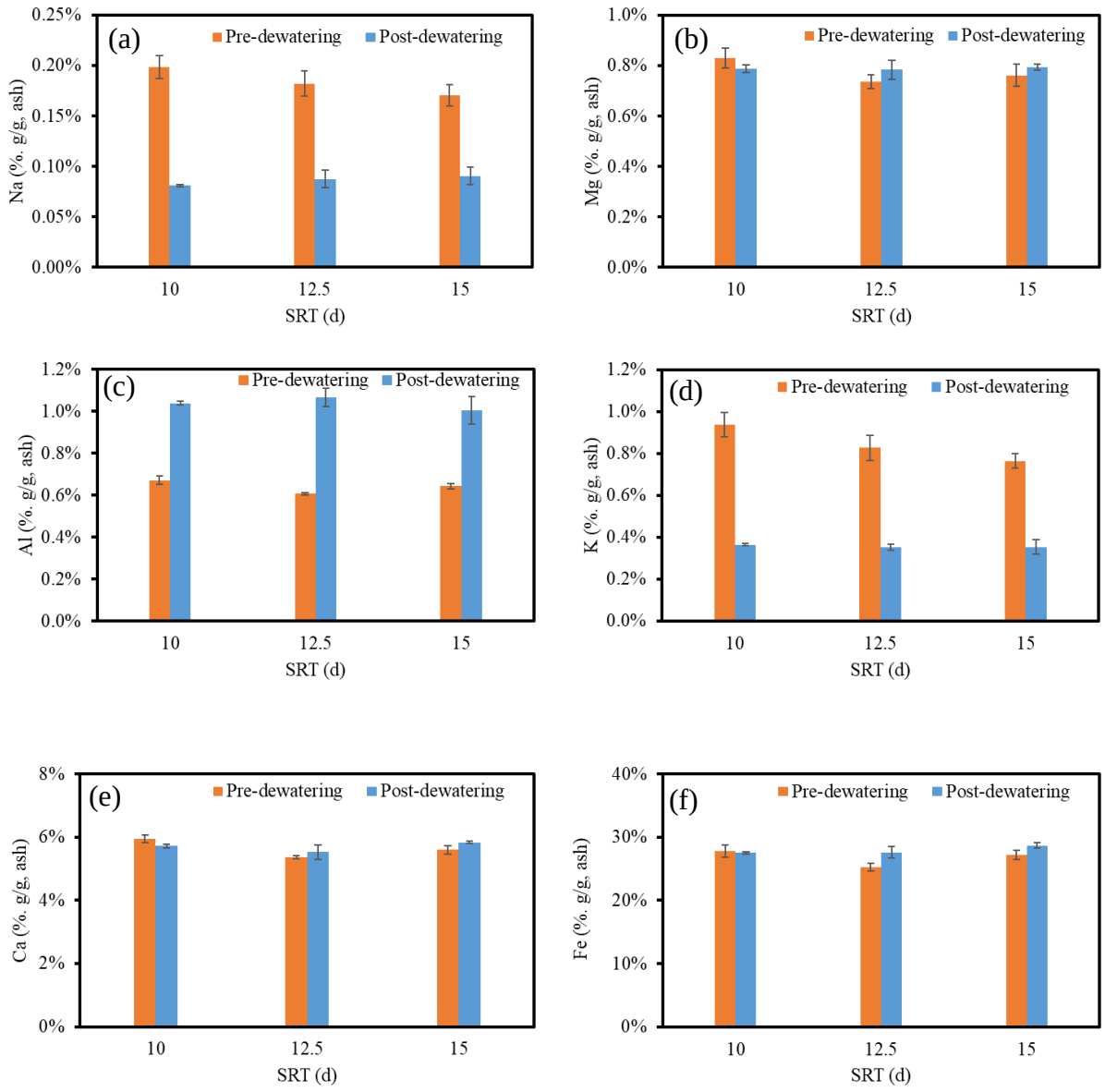

Figure 23. Sludge metal concentrations before and after dewatering at different SRTs

Table 6 . CHNS concentrations and BTU of dewatered cake

SRT (d)	CHNS (%, W/W, dry)				HHV
	C	H	N	S	(BTU/lb)
15	36.69%	4.9%	6.21%	1.11%	6920
12.5	35.94%	4.74%	6.08%	1.07%	6780
10	37.73%	5.13%	6.36%	1.08%	7180

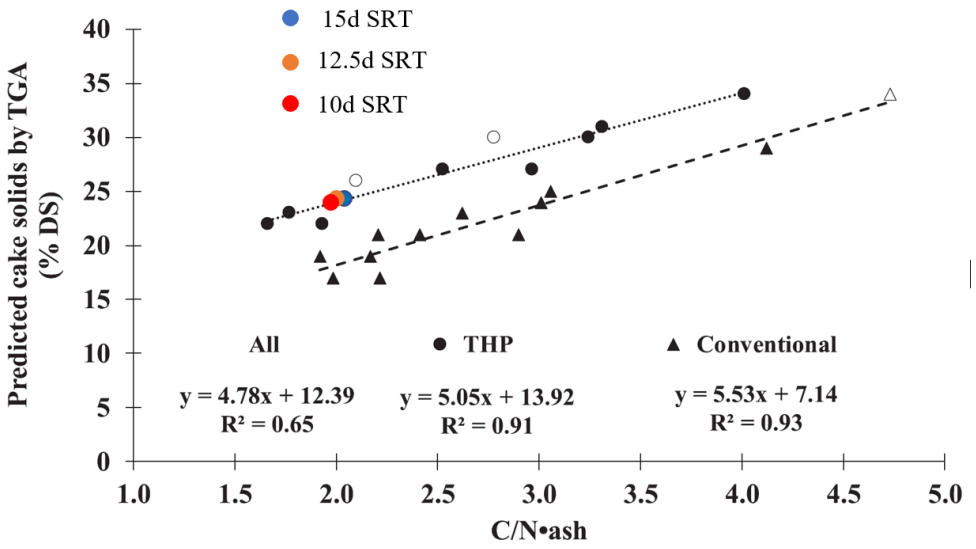

Figure 24. A comparison of C/N·ash values in this study and a previous study (Svennevik et al., 2019).

Table 7. 503 metal concentrations of dewatered cake

Metals	Concentrations (%, mg/kg, dry)			Limitations (%, mg/kg, dry)
	15d	12.5d	10d	
Arsenic	2.62	2.57	2.22	75
Cadmium	0.67	0.7	0.66	85
Chromium	107.72	111	62.33	3000
Copper	331.24	345.97	310.11	4300
Lead	9.73	10.92	10.51	840
Mercury	1.56	2.43	1.48	57
Molybdenum	17.03	15.51	11.74	75
Nickel	38.15	40.65	18.31	420
Selenium	2.45	2.57	2.22	100

Zinc	585.95	590.28	554.55	7500

3.3.5 Filtrate characterization

As shown in Figure 25, 98% TP, 50% OP, and 90% DOP have been retained in the dewatered cake, leaving 50% of OP and 10% DOP in filtrate (Figure 25). Likewise, around 95% tCOD and 60% sCOD were retained in the dewatered cake, leaving 5% tCOD and 40% sCOD in the filtrate (Figure 26). Besides, over 60% TKN, 50% sTKN, 65% DON, and 30% TAN were also retained in the cake, as well (Figure 27). The filtrates contain around 2000 mg/L sCOD, 1300 mg/L sTKN, 50-100 mg/L DON, 1300 mg/L ammonia, 10 mg/L OP, 10 mg/L DOP, 300 mg/L VSS, and 450mg/L SS (Figures 25, 26, 27, and 28).

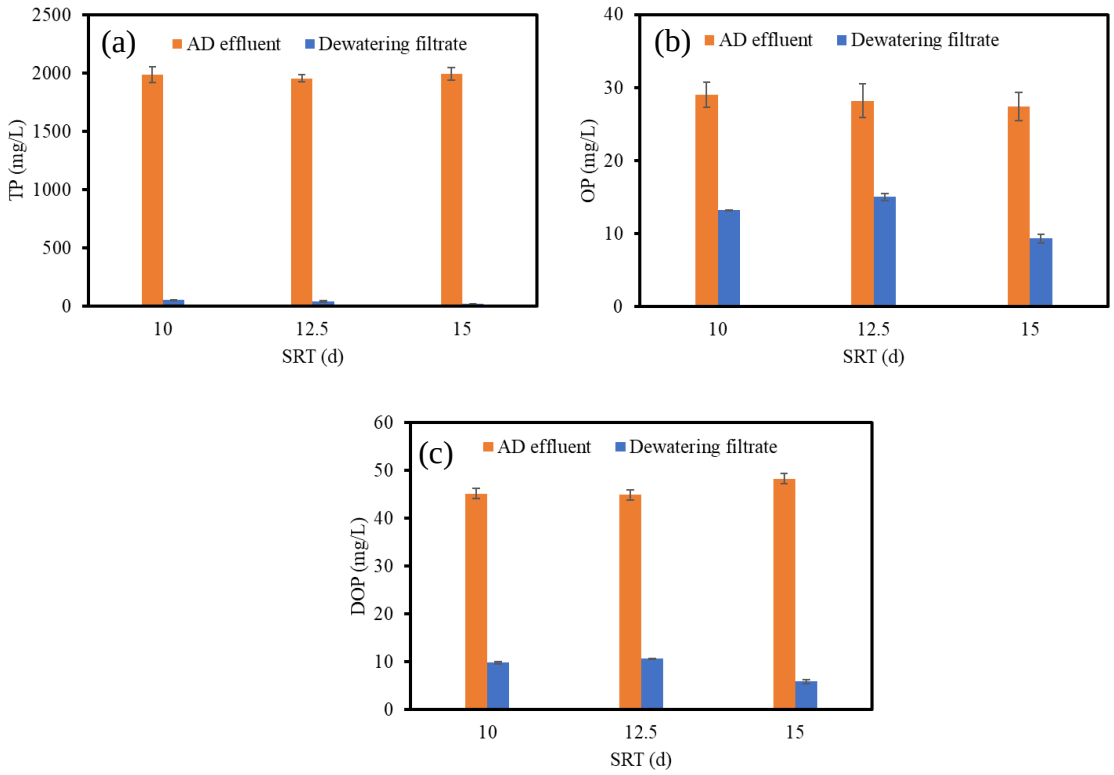

Figure 25. Sludge (a) TP, (b) OP, and (c) DOP concentrations before and after dewatering

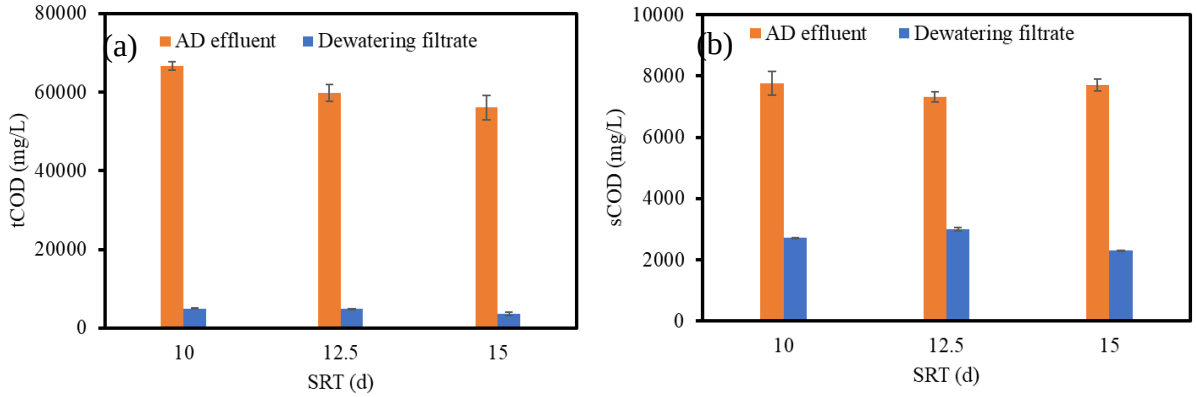

Figure 26. Sludge (a) tCOD and (b) sCOD concentrations before and after dewatering

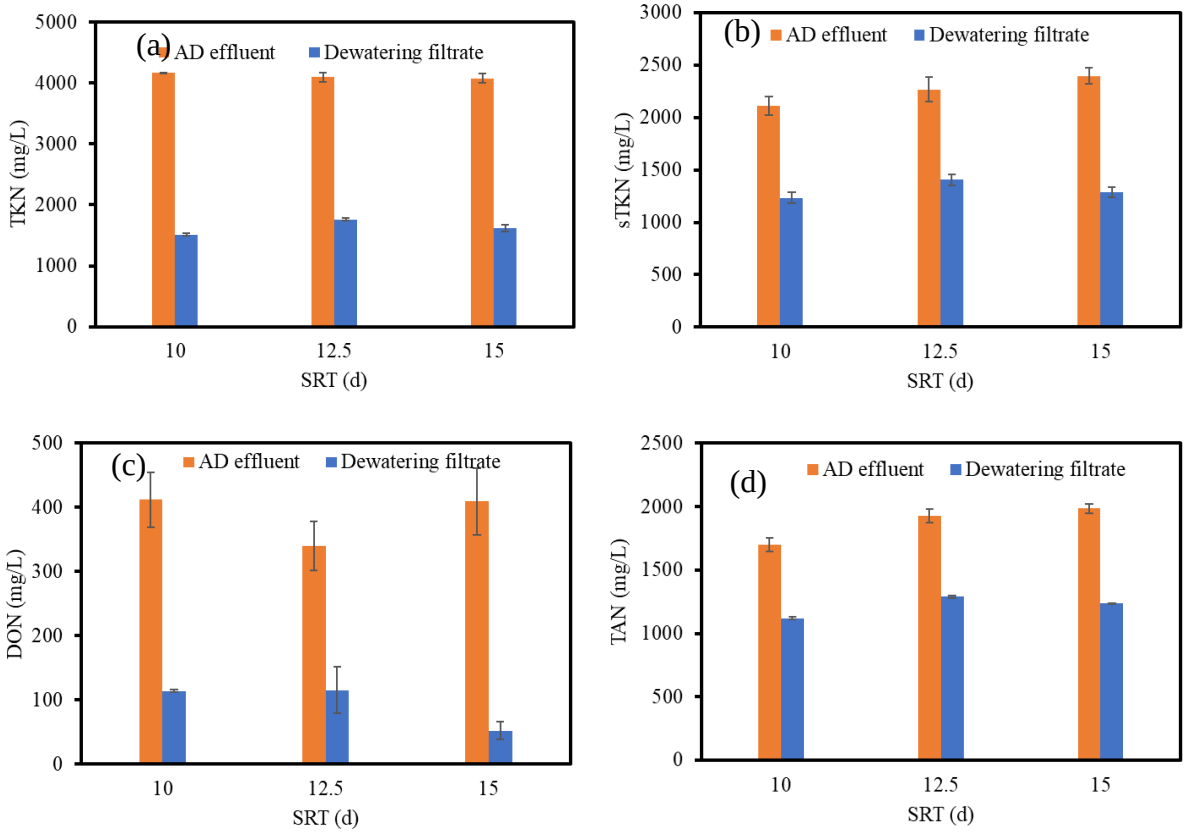

Figure 27. Sludge (a) TKN, (b) sTKN, (c) DON, and (d) TAN concentrations before and after dewatering

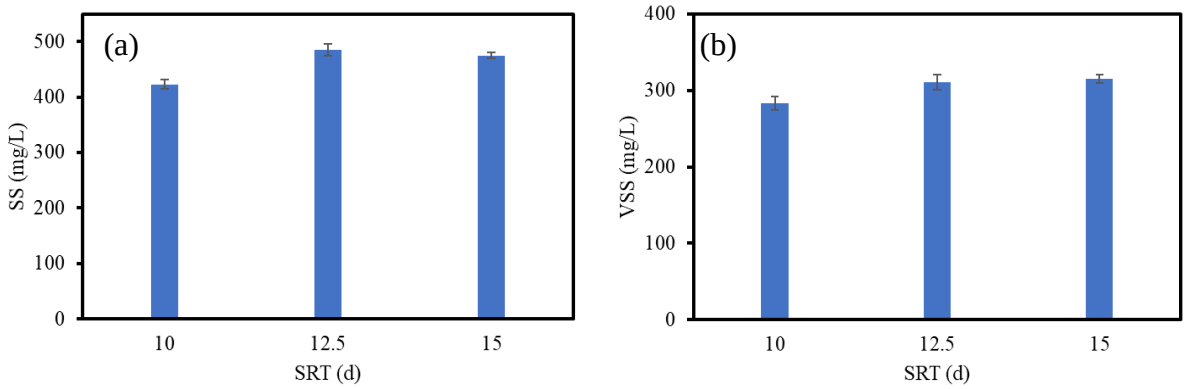

Figure 28. Filtrate (a) SS and (b) VSS concentrations

4 Conclusions

Following concluding remarks can be drawn from this project:

1. Reducing SRT from 15d to 10d reduced the TSR, VSR, and methane yield of the THP-pretreated sludge by 2 to 7%.
2. Sludge particle size and viscosity were reduced after THP and then further reduced after anaerobic digestion as a result of both thermal hydrolysis and biological degradation. In contrast, sludge CST values increased five fold after anaerobic digestion, indicating the poor dewaterability of sludge after anaerobic digestion. Mechanical mixing reduced the volume expansion from 8-15% to around 2% during ADs operation at different SRTs.
3. Biogas composition test results indicated that sulfur and siloxane compounds were insignificant and negligible in biogas.
4. TS of the dewatered cake was predicted to be around 25% for all three ADs, which is still lower than we expected. Low C/N ratios of the sludge in this study might be one of the causes of the poor dewaterability. All the 503 metal concentrations were lower than the permissible limits.
5. Very similar results were obtained between Bucknell's centrifuge dewatering methods and VT's piston methods in terms of OPD values and cake dryness.

5 References

APHA (2012) Standard methods for the examination of water and wastewater, 22 nd. Washington DC, American Public Health Association.

Bartek, N., Higgins, M.J., Murthy, S.N., Beightol, S. and Al-Omari, A. 2017. Understanding the Role of Mixing and Viscosity in Rapid Volume Expansion Due to Gas Holdup in Anaerobic Digesters. Proceedings of the Water Environment Federation 2017(1), 1-11.

Bougrier, C., Delgenès, J.P. and Carrère, H. 2008. Effects of thermal treatments on five different waste activated sludge samples solubilisation, physical properties and anaerobic digestion. Chemical Engineering Journal 139(2), 236-244.

Higgins, M., Bott, C., Schauer, P. and Beightol, S. 2014. Does Bio–P Impact Dewatering after Anaerobic Digestion? Yes, and not in a good way! Proceedings of the Water Environment Federation 2014(2), 1-11.

Jolis, D. 2008. High-Solids Anaerobic Digestion of Municipal Sludge Pretreated by Thermal Hydrolysis. Water Environment Research 80(7), 654-662.

Liu, X., Lee, C. and Kim, J. 2020. Thermal hydrolysis pre-treatment combined with anaerobic digestion for energy recovery from organic wastes. Journal of Material Cycles and Waste Management 22(5), 1370-1381.

Luo, H., Sun, Y., Taylor, M., Nguyen, C., Strawn, M., Broderick, T. and Wang, Z.W. 2022. Impacts of aluminum-and iron-based coagulants on municipal sludge anaerobic digestibility, dewaterability, and odor emission. Water Environment Research 94(1), e1684.

Luo, H., Zhang, D., Taylor, M., Nguyen, C. and Wang, Z.W. 2021. Aeration in sludge holding tanks as an economical means for biosolids odor control—A case study. Water Environment Research.

Management, U.S.E.P.A.O.o.W. (1994) A plain English guide to the EPA part 503 biosolids rule, US Environmental Protection Agency, Office of Wastewater Management.

Miryahyaei, S., Olinga, K., Muthalib, F.A., Das, T., Ab Aziz, M.S., Othman, M., Baudez, J.-C., Batstone, D. and Eshtiaghi, N. 2019. Impact of rheological properties of substrate on anaerobic digestion and digestate dewaterability: New insights through rheological and physico-chemical interaction. Water research 150, 56-67.

Novak, J.T., Sadler, M.E. and Murthy, S.N. 2003. Mechanisms of floc destruction during anaerobic and aerobic digestion and the effect on conditioning and dewatering of biosolids. Water Research 37(13), 3136-3144.

Ruiling, G., Shikun, C. and Zifu, L. 2017. Research progress of siloxane removal from biogas. International Journal of Agricultural and Biological Engineering 10(1), 30-39.

Shi, X., Zhu, L., Li, B., Liang, J. and Li, X.Y. 2021. Surfactant-assisted thermal hydrolysis off waste activated sludge for improved dewaterability, organic release, and volatile fatty acid production. Waste Management 124, 339-347.

Svennevik, O.K., Beck, G., Rus, E., Westereng, B., Higgins, M., Solheim, O.E., Nilsen, P.J. and Horn, S.J. 2019. CNash-A novel parameter predicting cake solids of dewatered digestates. Water research 158, 350-358.

Wang, X., Andrade, N., Shekarchi, J., Fischer, S.J., Torrents, Al. and Ramirez, M. 2018. Full scale study of Class A biosolids produced by thermal hydrolysis pretreatment and anaerobic digestion. Waste Management 78, 43-50.

Yang, G., Zhang, P., Zhang, G., Wang, Y. and Yang, A. 2015. Degradation properties of protein and carbohydrate during sludge anaerobic digestion. Bioresource technology 192, 126-130.

Zhang, D., An, Z., Strawn, M., Broderick, T., Khunjar, W. and Wang, Z.-W. 2021a. Understanding the formation of recalcitrant dissolved organic nitrogen as a result of thermal hydrolysis and anaerobic digestion of municipal sludge. Environmental Science-Water Research & Technology 7(2), 335-345.

Zhang, D., Santha, H., Pallansch, K., Novak, J.T. and Wang, Z.-W. 2020. Repurposing pre-pasteurization as an in situ thermal hydrolysis pretreatment process for enhancing anaerobic digestion of municipal sludge: a horizontal comparison between temperature-phased and standalone thermophilic or mesophilic anaerobic digestion. Environmental Science: Water Research & Technology 6(12), 3316-3325.

Zhang, W., Dong, B., Dai, X. and Dai, L. 2021b. Enhancement of sludge dewaterability via the thermal hydrolysis anaerobic digestion mechanism based on moisture and organic matter interactions. Science of The Total Environment 798, 149229.